THE USE OF CUMULUS ENSEMBLE MODELS TO STUDY THE PARAMETRISATION OF DEEP CONVECTION

D.GREGORY

HADLEY CENTRE, UK MET. OFFICE,
BRACKNELL, UK.

(Authors comment : much of the work reported here was carried out while the author was studying in the Atmospheric Physics Group at Imperial College, London and has been previously published in Gregory and Miller (1989). The reader is refered there for a more detailed report of the work.)

1. INTRODUCTION

It has long been stated that an aim of the development of meso-scale cloud models was to facilitate the development of convective parametrisation schemes for use in large-scale models of the atmosphere. One wonders whether this statement is akin to the 'greening' of research proposals today, for few studies to date have been specifically related to convective parametrisation. Most have studied the microphysics and dynamics of single clouds whereas convective parametrisation requires an understanding of the statistical properties of an ensemble of clouds and the relationship of those properties to the large-scale environment in which the cloud exist. However, having made this observation, it is true that these models would seem to provide a powerful tool for the development of convection schemes.

To date most studies to aid the development of convection schemes have been observational in nature, relying upon the few detailed observational data sets of convective atmospheres available (e.g. GATE, AMTEX, SESAME). Although details of the large-scale circulation can be obtained from field experiments, the properties of the clouds within this circulation are not easily obtained, at least over a sufficient sample to define the mean interaction of convection and the large-scale. Using budget techniques the overall effect of convection upon the large-scale flow may be diagnosed but the properties of clouds and the effect of their various components (updraughts and downdraughts) upon the large-scale flow cannot be inferred directly. To overcome these difficulties many authors have attempted to use simple one-dimensional cloud models (Yanai et al 1973, Johnson 1980), essentially using a mass flux convection scheme in a diagnostic mode. However these simple models are crude; microphysics are poorly represented, many do not contain a downdraught representation or the organisational effects of shear. There seems also a danger in such techniques

in that a convection scheme is being used to verify a convection scheme! The limited amount of observational data of sufficient quality on which such budget studies can be carried out also means that convection schemes can only be verified in detail against a small range of situations, whereas there is known to be great variety in the nature of convective instability around the globe.

Convective scale models have several advantages over such 'observational techniques'. Clouds are explicitly modelled and able to respond to the thermodynamic and dynamic structure of the atmosphere in a realistic manner. Because greater details of the convective process can be obtained a more detailed analysis of the impact of convection upon the large-scale flow can be carried out. Also the response of convection to a wider range of atmospheric states and forcing may be studied. Of course in order to study the 'statistical' impact of convection, models in which more than one cloud exists are needed. Such cumulus ensemble models (CEM) require domains several hundred kilometers in length, with horizontal resolutions of 1km or greater. Because of these criteria such models to date have tended to be two-dimensional. The first such model was developed by Hill (1974) but with a rather limited domain (30km in length). Since then domain sizes have increased and the use of limited three-dimensional convection models has now become possible (Tao et al(1987) - 32×32km domain)

This paper discusses the simulation of an ensemble of deep tropical clouds over the GATE area under the influence of observed large-scale forcing using such a cumulus ensemble model. It is shown that such a model can realistically represent the observed properties of an ensemble of clouds. Using the results from this model the problem of convective parametrisation is studied, mainly from a mass flux scheme perspective. The control of convection by large-scale forcing and thermodynamic structure is also considered.

2. THE THEORY OF CONVECTIVE PARAMETRIZATION

The area averaged form of the equations of fluid dynamics are well known. In pressure co-ordinates those for potential temperature (θ) and mixing ratio (q) averaged over an area A are (in two dimensions and flux form),

$$\frac{\partial \bar{\theta}}{\partial t} + \overline{\frac{\partial u\theta}{\partial x}} + \overline{\frac{\partial \omega\theta}{\partial p}} = \left\{ \frac{L\bar{Q}}{c_p \pi} - \overline{\frac{\partial \omega'\theta'}{\partial p}} + \overline{S_\theta} \right\} - \frac{Q_{RAD}}{\pi}$$

$$= \frac{Q1}{\pi} - \left[\overline{\frac{\partial \omega'\theta'}{\partial p}}\right]_{BL} + \overline{S_\theta} - \frac{Q_{RAD}}{\pi} = \frac{Q1_{TOT}}{\pi} - \frac{Q_{RAD}}{\pi} \qquad (1)$$

$$\frac{\partial \bar{q}}{\partial t} + \overline{\frac{\partial uq}{\partial x}} + \frac{\partial \bar{\omega}\bar{q}}{\partial p} = \{ - \bar{Q} - \frac{\partial \overline{\omega' q'}}{\partial p} + \overline{S_q} \} = Q2 - [\frac{\partial \overline{\omega' q'}}{\partial p}]_{BL} + \overline{S_q} = Q2_{TOT} \quad (2)$$

where $\varphi = \bar{\varphi} + \varphi'$

$-Q$ is the moisture sink/source due to moist processes

$(\varphi)_{BL}$ is the forcing due to surface processes

Q_{RAD} is the radiational heat source/sink

S_φ are turbulent tendencies

and π is $(p/p_o)^{R/c_p}$

$Q1_{TOT}$ and $Q2_{TOT}$ are termed the apparent heat source and apparent moisture source due to diabatic processes (Yanai et al 1973). For the purposes of this paper Q1 and Q2 represent the contribution of convection to these quantities. In parametrisation Q1 and Q2 must be estimated in terms of grid point values of a numerical model. This can be achieved by expressing Q1 and Q2 in terms of large-scale and cloud-scale variables (Ooyama 1971; Arakawa and Schubert 1974). This technique is outlined below.

The area averaged value of any quantity (φ) can be expressed as a mean of the quantity over cloudy air $(\bar{\varphi}^c)$ and clear air $(\bar{\varphi}^e)$ weighted by the area covered by each;

$$\varphi = \sigma(\bar{\varphi}^c) + (1-\sigma)(\bar{\varphi}^e) \quad (3)$$

where σ is the fractional cloud area within an area A.

Using eqn(3) the vertical eddy flux can be written as,

$$\begin{aligned} \overline{\omega'\phi'} &= \overline{\omega\phi} - \bar{\omega}\bar{\phi} \\ &= (\sigma\ \overline{\omega\phi}^c + (1-\sigma)\ \overline{\omega\phi}^e) - (\sigma\bar{\omega}^c + (1-\sigma)\ \bar{\omega}^e)\ \bar{\phi} \\ &= (\sigma\ \overline{\omega\phi}^c - \sigma\ \bar{\omega}^c\ \bar{\phi}) + ((1-\sigma)\ \overline{\omega\phi}^e - (1-\sigma)\ \bar{\omega}^e\ \bar{\phi}) \end{aligned} \quad (4)$$

The second term of the r.h.s of eqn(4) is usually neglected as $\omega^c \gg \omega^e$ and also because $\sigma \ll 1$, $\bar{\varphi}^e \simeq \bar{\varphi}$ for θ and q.

Following on from this $\bar{Q}^e$ is determined by consideration of the θ and q equations averaged over cloudy air. After some manipulation Q1 can be expressed as,

$$Q1 = (1-\sigma)\ \frac{L\bar{Q}^e}{c_p \pi} + \{ \sum_{\substack{\text{detraining} \\ \text{cloud}}} D_i\ (\bar{\theta}_i^c - \bar{\theta}) \} + \sigma\bar{\omega}^c\ \frac{\partial \bar{\theta}}{\partial p} \quad (5)$$

and similarly for Q2.

Here D_i is the detrainment rate for cloud type i; φ_i is φ for cloud type i; $\sigma\omega^c$ is the mass flux averaged over all cloud and $\bar{Q}^e$ is the evaporation of water within the cloud environment. In a parametrization scheme such quantities are determined through the use of simple analytical cloud models.

In this paper the expressions for Q1 and Q2 are analysed using a meso-scale convection model to determine which are the most important terms. Using cloud quantities from the model, approximations used by previous workers in the derivation of expressions for Q1 and Q2 are not required; namely assumptions of steady-state and constant cloud area with height. Also because the model resolves the flow across cloud boundaries approximations used to describe entrainment and detrainment processes need not be made. Hence a fuller analysis may be carried out. Full details are to be found in Gregory and Miller (1989) where it is shown that Q1 can be expressed as,

$$Q1 = (1-\sigma)\frac{L\bar{Q}^e}{c_p\pi} + (\bar{\theta} - \theta_b)\frac{\partial\sigma}{\partial t} + \frac{\partial\sigma\bar{\theta}^c}{\partial t} + (\omega_b\bar{\theta} - (\omega\theta)_b)\frac{\partial\sigma}{\partial p} + \sigma\left(\overline{u\frac{\partial\theta}{\partial x}}\right)^c + \sigma\left(\overline{\frac{\partial u}{\partial x}(\theta-\bar{\theta})}\right)^c + \sigma\,\bar{\omega}^c\frac{\partial\bar{\theta}}{\partial p} - \sigma\,\bar{S}_\theta^c \qquad (6)$$

and similarly for Q2 (φ_b is the value of φ at the cloud boundary).

In both the approximate and full forms, convection is seen to modify its environment through compensating subsidence. However transports across cloud boundaries differ because of the representation of entrainemnt and detrainment in the simple cloud models used to derive the approximate forms. Terms due to the time dependent nature of the ensemble and the fact that cloud area varies with height are also present in the fuller form.

The momentum equation can be treated in a similar manner, the area averaged equation in two-dimensions being,

$$\frac{\partial\bar{u}}{\partial t} + \frac{\partial\overline{u^2}}{\partial x} + \frac{\partial\bar{\omega}\bar{u}}{\partial p} + g\,\overline{\frac{\partial h}{\partial x}} = -\frac{\partial\overline{\omega'u'}}{\partial p} + \overline{S_u} \qquad (7)$$

neglecting hozizontal eddy transports and the Coriolis term. The pressure gradient on the l.h.s of the equation contains both mean and eddy terms. The eddy transport term of eqn(7) is often termed 'cumulus friction' (Schneider and Lindzen 1976) and is here denoted by Q3. Following the method outlined above an expression for Q3 in terms of cloud and large-scale variables can be written as,

$$Q3 = \frac{\partial \sigma \bar{u}^c}{\partial t} + (\bar{u}-u_b)\frac{\partial \sigma}{\partial t} + [\omega_b \bar{u} - (\omega u)_b]\frac{\partial \sigma}{\partial t} + \sigma\left(\overline{u\frac{\partial u}{\partial x}}\right)^c$$

$$+ \sigma\left(\overline{\frac{\partial u}{\partial x}(u-\bar{u})}\right)^c + g\sigma\left(\overline{\frac{\partial h}{\partial p}}\right)^c + \sigma\bar{\omega}^c\frac{\partial \bar{u}}{\partial p} - \sigma \bar{S}_u^c \qquad (8)$$

This is identical to the expression for Q1 above except for the inclusion of the effects of cloud scale pressure gradients upon the large-scale flow.

Although the full expressions for Q1, Q2 and Q3 are too complicated to be used in a convective parametrization scheme, using data from a numerical cloud model each term can be diagnosed to investigate which are important and whether the approximate forms are adequate to represent convective processes in large-scale models accurately.

3. SIMULATION OF CONVECTION IN A GATE EASTERLY WAVE

3.1 Model description

The model used is based upon that described by Miller and Pearce (1974), although some modifications have been included since it was originally developed (see Gregory and Miller (1989)). Only warm microphysics are included based upon the ideas of Kessler (1969). A two dimensional cyclic domain, 256km in length is used with a horizontal resolution of 1km. Pressure co-ordinates are used in the vertical with a resolution of 50mb (between 1000 and 100mb).

Several experiments were carried out using data from the composite GATE easterly wave data set of Thompson et al (1979) (hereafter referred to as TPRR) (table 1). Two initial data times were used; 2 hours and 20 hours after the passage of the ridge of an easterly wave across the GATE area. The imapct of large-scale horizontal advection and vertical ascent upon the models thermodynamic profiles were represented by heating and moistening rates added to the models thermodynamic and specific humidity equations, values being based upon those of TPRR and updated every two hours to simulate the passage of an easterly wave through the domain. Radiative cooling was similarly modelled using the profile for the GATE area due to Cox and Griffith (1979). Surface fluxes of sensible and latent heat were fixed throughout each simulation but varied with the time of the initial conditions used. For simulations starting 2 hours after the ridge of the wave had passed over the GATE area values were 5 and 89Wm^{-2} respectively, while those starting at 20 hours use 10 and 125Wm^{-2}.

SIMULATION	TIME OF INITIAL CONDITIONS		TIME OF LARGE-SCALE FORCING	COMMENTS
	T, q	u		
A	20hr	no wind	20-30hr	Main simulation
B	20hr	no wind	0-10hr	To study the problem of moisture storage
C	2hr	no wind	0-10hr	
D	20hr	20hr	20-30hr	To study the parameterization of momentum transports
E	20hr	2hr	20-30hr	

Table 1 Summary of experiments

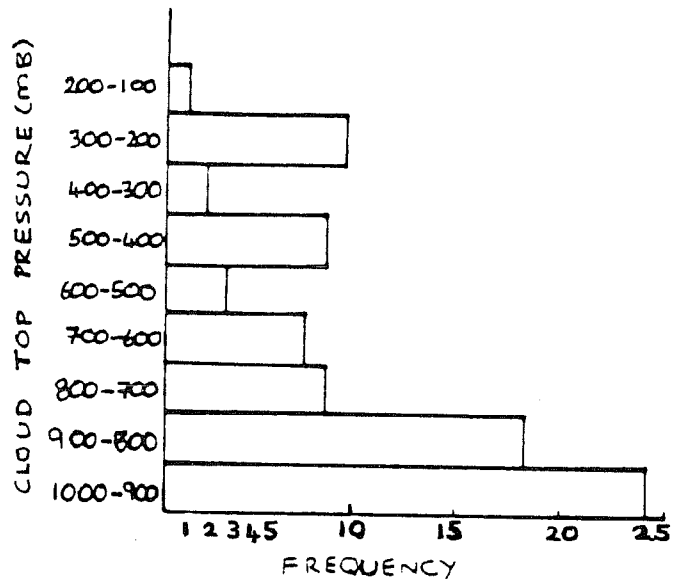

Fig. 1 Cloud top height population

These were distributed over the two lowest model layers to simulate the effects of boundary layer mixing.

In each simulation the model was integrated forward for nine hours. Convection was initiated by random heating perturbations with a horizontal scale of 4km applied at 925 and 875mb. These aim to represent the forcing of deep convection by shallow convection in the boundary layer. The heating rates range from -0.12 to 0.12K/minute and were kept fixed for a period of 30 minutes. It was necessary to maintain the forcing over the whole nine hours of the simulation for convection to continue to develop, but probably less so in those with an initial horizontal wind where the interaction of gust fronts and the wind field aid the development of further convection. In all simulations the net contribution of the forcing to the models energy budget is near zero.

3.2 Simulation A : 20 - 30 hours of TPRR wave cycle

Thermodynamic profiles and forcing from 20 hours after the ridge of an easterly wave had passed over the GATE area were used. No initial wind profile was included. Deep convection forms after the first hour of the integration. A variety of differing size clouds are present (fig 1), some only reaching the mid-troposphere before loosing buoyancy while others have tops around 200mb. There they spread out laterally to form 'anvil' clouds merging with the remnants of previous clouds. These are not anvils in the true sence, being only 200mb thick and composed of water, not ice (the model microphysics does not represent ice). No rain is associated with these features, the cloud liquid water content not exceeding the 0.5g/kg required for the auto-conversion of cloud to rain water.

The cloud top height spectrum seen within the model is continuous to 600mb with peaks above this between 500 and 400mb and 200 and 300mb, agreeing with the levels of large-scale horizontal divergence over the GATE area (fig 3 of TPRR). The gap that exists in the spectrum between deep and medium level convection is due to the formation of a warm, dry layer in mid-levels due to deep convection.

The observed and simulated energy budgets are compared in table 2. The eight hour average (between one and nine hours) is in good agreement with observations, considering that errors of up to 20% exist in these (TPRR). The vertical distribution of $Q1_{TOT}$ and $Q2_{TOT}$ is in reasonable agreement with that

SENSIBLE HEAT

Time (hr)	LS forcing, radiative cooling (Wm^{-2})	Cloud and boundary layer forcing (Wm^{-2})	$\langle c_p \pi Q1 \rangle$ (Wm^{-2})	
			Observed	Simulated
1-9	-666	-3	676	527

LATENT HEAT

Time (hr)	LS forcing, radiative cooling (Wm^{-2})	Cloud and boundary layer forcing (Wm^{-2})	$\langle LQ2 \rangle$ (Wm^{-2})		Surface rainfall (Wm^{-2})	
			Observed	Simulated	Observed	Simulated
1-9	548	127	-635	-527	557	523

Table 2 Comparison of the energy budget of simulation A with observations.

observed (fig 2). Too little heating occurs above 500mb, perhaps owing to the absence of meso-scale precipitation features in the simulation. With a high-resolution cloud model the components of $Q1_{TOT}$ and $Q2_{TOT}$ (condensational heating/evaporative cooling, eddy flux divergence, turbulence effects) can be diagnosed (fig 3). For both turbulence effects are negligible. Vertical eddy flux divergence plays a more important role in determining $Q2_{TOT}$ than $Q1_{TOT}$. For $Q1_{TOT}$, vertical eddy transports play a secondary role, redistributing energy from below 600mb to higher levels. For $Q2_{TOT}$ moist and eddy processes play more of an equal role, eddy transports dominating moist processes in the lowest 300mb. However the transport of moisture out of the lowest 200mb appears to be too large causing excessive drying compared to observation. These suggest a drying of the lowest 200mb by 0.3g/kg in the first 3 hours of the simulation whereas the model produces a drying of 1.25g/kg in the same period. This appears to be a consequence of using a two-dimensional domain.

4. THE PARAMETRISATION OF CONVECTION

Cumulus parametrisation involves two problems. The first, to obtain a reasonable estimate of the vertical distribution of heating and moistening due to convection is considered in sections 4.3.1 and 4.3.2. Aspects of the second part, the closure problem, are addressed in section 5. The parametrisation of momentum transports will be considered in section 6.

4.1 Defining updraughts and downdraughts

The parametric expressions for Q1 and Q2 derived in section 2 contain cloud variables. Using a cumulus ensemble model it is difficult to specify properties of each type of cloud in the ensemble. Hence in the following discussion the 'mean ensemble cloud' is defined by averaging over all cloudy air on a pressure level. In parmetrisation, the mean effect of the clouds is required and so the mean ensemble cloud proves a useful concept.

Updraught and downdraught are defined by:

updraught (UD)	$W \geq 1$m/s	and q_C or $q_R \geq 0.1$g/kg
downdraught (DD)	$W < 0$	and $q_R \geq 0.1$g/kg

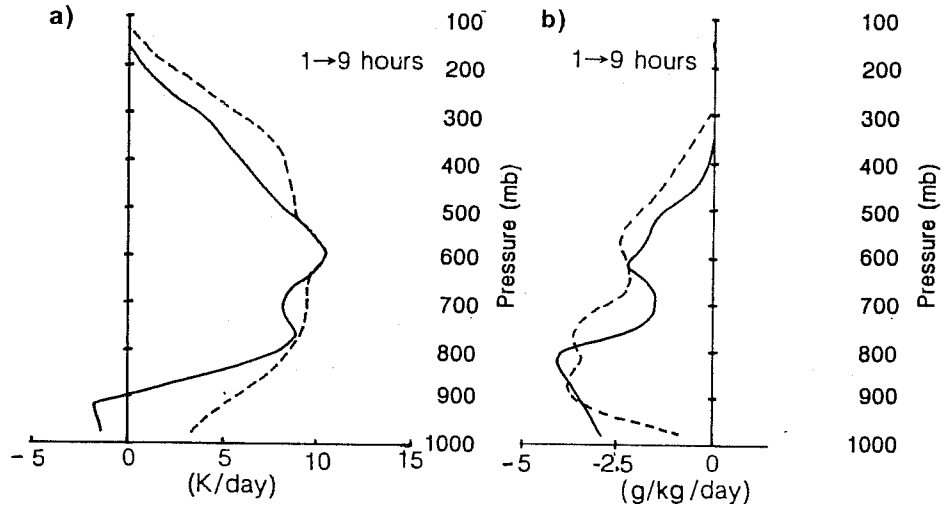

Fig. 2 Vertical distribution of the modelled (——) (a) $Q1_{TOT}$ and (b) $Q2_{TOT}$ compared with observed values (- - - -) for simulation A.

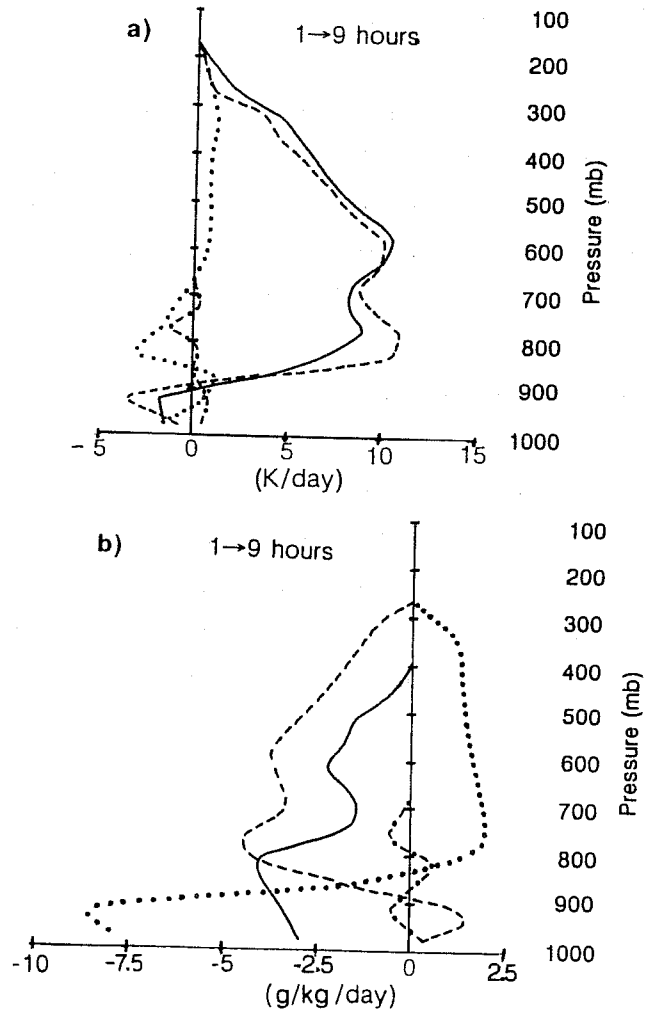

Fig. 3 Contribution of condensational heating/evaporative cooling (- - - -), vertical eddy flux divergence (.....) and turbulent effects (-.-.-.-) to (a) $Q1_{TOT}$ and (b) $Q2_{TOT}$ (——) for simulation A (contribution of boundary layer forcing not shown).

where q_C is the cloud water content and q_R is the rainwater content. Convective downdraughts are usually associated with large concentrations of rainwater and so only this is considered in definition.

Each grid point of the model is tested using the above conditions to build up the average vertical profile of these features. Any cloudy air not satisfying the above conditions is termed inactice cloud (IC).

4.2 Vertical mass flux

An important quantity in the parametric forms for Q1 and Q2 is the area-averaged cloud mass flux ($\sigma\tilde{\omega}^C$). Figure 4 shows this for the three components of cloud defined above. Updraught mass flux peaks around 750mb with inflow occurring below this and a deep outflow layer above (presumably from different height clouds). Below 800mb the contribution of inactive cloud is important. Although vertical velocities in such cloud are small on average they cover 12% of the domain at low levels, mainly associated with the inflow into deep convection. Downdraughts have a different profile shape to that of the updraughts with a deep entrainment layer above 800mb and a shallow outflow layer near the surface. Above 800mb, downdraught mass flux is approximately half the magnitude of that of updraughts, showing its importance in defining the net convective mass flux. These values are similar to the two- and three-dimensional results of Tao et al. (1987).

These results contrast with the mass flux profiles obtained from analytical cloud models used in many parametrization schemes (e.g. fig 4 of Anthes 1977), in which updraughts are represented by entraining plumes. Entrainment of air is assumed to occur up to the zero buoyancy level with only a thin detrainment layer at cloud top with mass flux peaking just below this. The modelled peak at 750mb is influenced by the presence of medium height convection. Study of individual deep convective clouds within the domain shows $\sigma\omega^{UD}$ peaking in mid-levels. Many analytical cloud models do not consider the effects of downdraughts. However, the simulation shows their importance in determining the net convective mass flux. When included in simple models they are represented by inverted plumes with a shallow detrainment layer near the surface. This would seem reasonable as $\sigma\omega^{DD}$ increases gradually from cloud top towards the surface.

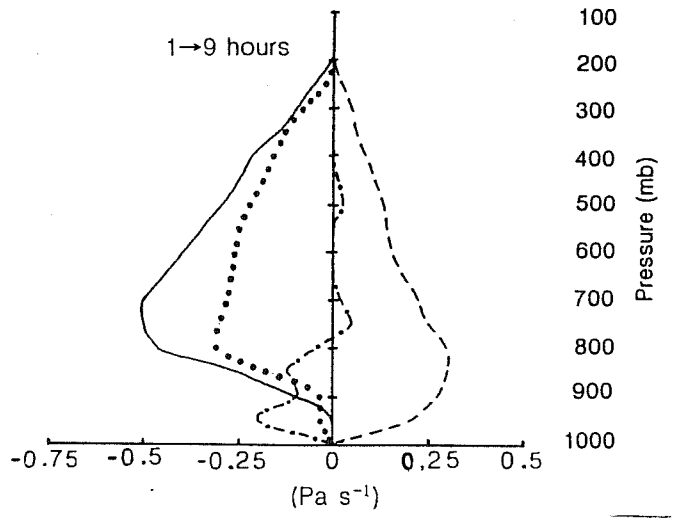

Fig. 4 Profiles of $\sigma\bar{\omega}^c$ for updraught (UD) (——), downdraught (DD) (- - - -), inactive cloud (IC) (-·-·-·-) and all cloudy air (·····) for simulation A.

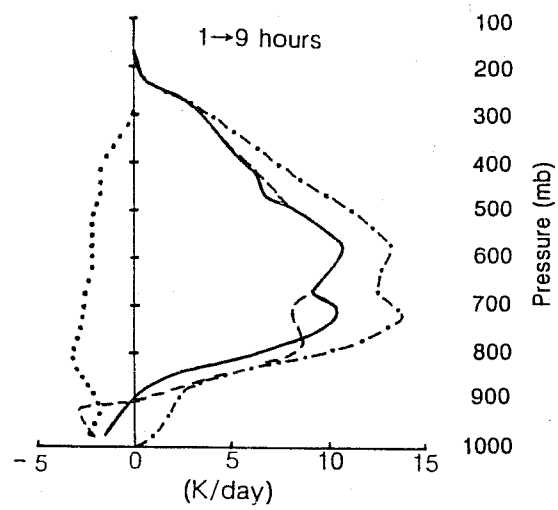

Fig. 5 Profiles of $(CS)_T$ (-·-·-·-), $(EE)_T$ (·····), $(CS+EE)_T$ (——) and Q1 (- - - -) for simulation A.

4.3 Vertical distribution of convective heating/moistening

In this section the sepecification of the vertical distribution of cumulus heating/moistening is considered. The parametric forms of Q1 and Q2 (eqn(6)) were diagnosed using the cumulus ensemble model. Further details of the procedure used are to be found in Gregory and Miller (1989).

4.3.1 Convective heating (Q1)

Table 3 presents budgets of the r.h.s of eqn(6) averaged between one and nine hours of simulation A. Values over all cloudy air and for each of the three cloud components are listed. In the following discussion terms are referred to by their abbreviations (listed in the table).

The three largest terms in the budget are those labelled BAL, which are at least one order of magnitude greater than Q1. However, on summation the net result is only 8% of Q1, the great degree of cancelation also being reflected in the vertical profiles (not shown). At any level of the model the net value never exceeds a few K/d, whereas individual terms are several hundred K/d. This balance arises because the terms involved are an approximate expression of the cloud-averaged continuity equation (see Gregory and Miller (1989) for further details). Parametrisation schemes neglect the BAL terms by assuming steady-state clouds and σ constant with respect to pressure. The numerical model results show that the consequences for cumulus parametrisation are small.

Figure 5 shows profiles of EE and CS, the next two largest terms in the budget (agreeing with observational studies). EE is usually attributed to the evaporation of detrained liquid water. The negative value of EE at all levels would agree with this, indicating that the time-dependent contribution is small (although $\partial\sigma/\partial t$ can be large, $(\bar{\theta}-\theta_b) \ll \theta$).

CS represents the response of the cloud environment to motions within cloud. Budget values indicate that CS for all cloudy air overestimates Q1 by ~ 30%. The vertical profile follows $\sigma\omega^c$ (fig 4), $\partial\bar{\theta}/\partial p$ being approximately constant with height throughout the cloud layer. For all cloud air CS has a similar vertical structure to Q1, overestimating it by 3K/d in the mid-troposphere and with no cooling being seen in the lowest 100mb. Adding EE to CS gives a budget value of $495 Wm^{-2}$ (only 5% less than Q1) and brings better agreement above 800mb. Below this, Q1 is underestimated by ~3K/d, although the cooling of the

TERM		ALL CLOUD (Wm^{-2})	UD (Wm^{-2})	DD (Wm^{-2})	IC (Wm^{-2})
$\pi\sigma\bar{\omega}^c\frac{\partial\bar{\theta}}{\partial p}$	(CS)	692	1026	-508	174
$(1-\sigma)(L\bar{Q}/c_p)^e$ + $\pi(\bar{\theta}-\theta_b)\partial\sigma/\partial t$	(EE)	-197	-	-	-
$\pi\sigma\overline{\left(\frac{\partial u}{\partial x}(\theta-\bar{\theta})\right)}^c$	(ED)	52	39	4	9
$\pi\sigma\overline{\left(u\frac{\partial\theta}{\partial x}\right)}^c$	(ADV)	-58	-17	-22	-19
$\pi\frac{\partial\sigma\bar{\theta}^c}{\partial t}$		11669	-104	1444	10329
$\pi\omega_b\bar{\theta}\frac{\partial\sigma}{\partial p}$	(BAL)	-19139	3659	-5250	-17548
$-\pi(\omega\theta)_b\frac{\partial\sigma}{\partial p}$		7427	-3537	3791	7173
$-\pi\sigma\bar{S}_\theta^c$	(TURB)	-17	24	-7	-34
$-\pi\sigma\left(\frac{\partial\theta}{\partial t}\right)_{FOR}$	(FORC)	98	3	28	67
$\pi(Q1)_{para}$		527	1093	-520	151
$\pi Q1$		527	-	-	-

Table 3 Budgets of terms on rhs of the parametric form of $(Q1)_{para}$ for all cloudy air, updraught (UD), downdraught (DD) and inactive cloud (IC) averaged between one and nine hours. Abreviations for terms used in text are indicated in brackets.

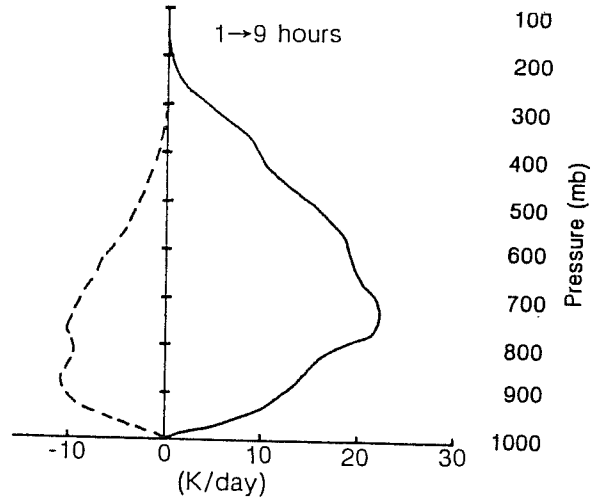

Fig. 6 Contribution of (UD+IC) (——————) and DD(- - - -) to $(CS)_T$ for simulation A.

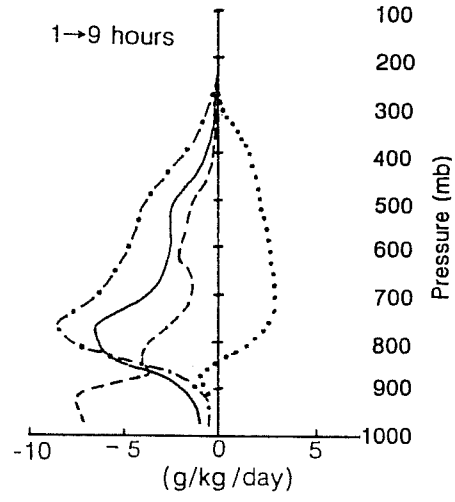

Fig. 7 Profiles of $(CS_{>q})$ (—·—·—·—), $(EE_{>q})$ (·····), $(CS+EE)_{>q}$ (——————) and Q2 (- - - -) for simulation A.

lowest model layer is reasonable. Thus a combination of CS and EE would seem to provide a good representation of Q1, confirming results of previous workers, who used analytical models to provide cloud variables (e.g. Yanai et al (1973)). However a word of caution must be introduced.

Many parametrization schemes do not include downdraughts, the mass flux they estimate being for updraught air only. These results indicate the importance of downdraughts in specifying both the magnitude and vertical structure of Q1. Figure 6 shows the contribution of subsidence due to updraughts plus inactive cloud and downdraughts. Budgets show that subsidence due to updraughts is approximately twice Q1, the profile peaking at 750mb, with a maximum of ~20K/d. CS due to downdraughts has a budget value similar to Q1, but is of opposite sign and has a lower maximum than that due to updraughts, being relatively flat between 700 and 900mb. Hence, subsidence due to updraught plus EE is a bad representation of Q1. The fact that, using updraughts only, previous workers have obtained reasonable representations of Q1, presumably indicates that the mass flux profiles used were questionable.

Other terms in the budget are small and contribute little to improving the representation of Q1.

4.3.2 Convective moistening (Q2)

Table 4 presents the budgets of the parametric form of Q2. The BAL terms have individual magnitudes of the order of Q2 and the cancellation is not as great as seen previously, the residual being ~15% of |Q2|.

EE has a budget value of ~15% of Q2 (similar to the Q1 budget). However, the contribution of the time dependent term is larger because the approximation $(q-q_b) \ll q$ is worse for moisture than for temperature. The profile of EE (fig 7) shows drying in the lowest 200mb, presumably associated with the time-dependent term. CS for all cloud overestimates Q2 by 50%, and the vertical profile does not represent the Q2 well. CS follows $\sigma\bar{\omega}^c$, which peaks at 775mb, the increase in $\partial q/\partial p$ towards the surface being insufficient to bring the maximum down to the observed level (925mb).

ED and ADV oppose each other, both being larger than in the Q1 budget. Their net value is negative implying that these processes dry the domain. With simple cloud models the entrainment and detrainment processes moisten the environment

TERM		ALL CLOUD (Wm^{-2})	UD (Wm^{-2})	DD (Wm^{-2})	IC (Wm^{-2})
$\sigma\bar{\omega}^{c}\frac{\partial\bar{q}}{\partial p}$	(CS)	-801	-1209	661	-252
$-(1-\sigma)\bar{Q}^{e}$ + $(\bar{q}-q_{b})\partial\sigma/\partial t$	(EE)	202	-	-	-
$\sigma\overline{\left(\frac{\partial u}{\partial x}(q-\bar{q})\right)}^{c}$	(ED)	-163	27	-92	-97
$\sigma\overline{\left(u\frac{\partial q}{\partial x}\right)}^{c}$	(ADV)	105	45	41	19
$\frac{\partial\sigma\bar{q}^{c}}{\partial t}$	(BAL)	364	<0	115	249
$\omega_{b}\bar{q}\frac{\partial\sigma}{\partial p}$	(BAL)	-859	654	-525	-988
$-(\omega q)_{b}\frac{\partial\sigma}{\partial p}$	(BAL)	571	-744	421	894
$-\sigma\bar{S}_{q}^{c}$	(TURB)	138	55	<0	83
$-\sigma\overline{\left(\frac{\partial q}{\partial t}\right)_{FOR}}^{c}$	(FORC)	-84	-10	-20	-56
$(Q2)_{para}$		-527	-1182	601	-148
Q2		-527	-	-	-

Table 4 Budgets of terms on rhs of the parametric form of $(Q2)_{para}$ for all cloudy air, updraught (UD), downdraught (DD) and inactive cloud (IC) averaged between one and nine hours. Abreviations for terms used in text are indicated in brackets.

through outflow of moist cloud air into the environment. With clouds simulated in the mesoscale model some detrainment moistening occurs above 800mb. However, the dominant effect is in the inflow layer where the large-scale atmosphere is dried. Simple cloud models assume that air entrained from the cloud environment has the same thermodynamic characteristics as the large-scale atmosphere and so contributes nothing to the effects of clouds upon their large-scale environment. In the model, the moisture fields surrounding the clouds in the inflow region is 1g/kg wetter than the domain average. Hence horizontal transports across the cloud boundary in the inflow layer dry the domain.

Is there a simple method to represent Q2 as with Q1? Using CS and EE gives a budget value of $-600 Wm^{-2}$, overestimating Q2 by about 15%. The vertical profile of this combination peaks at 775mb, with too little drying below and too much above. Addition of ADV and ED bring a little more drying to the surface but does not move the peak downwards. Addition of the vertical flux divergence of the neglected part of eqn(4) does bring more improvement below 800mb. This term is not negligible here because of weak dry motions induced by the cloud forcing in the cloud environment. The effect of these is similar to that of shallow convection (fig 8), at least for moisture. For temperature the heating is of the opposite sign because of the lack of evaporation of condensed water detrained into the environment from non-precipitating clouds. These results suggest that shallow convection is important in specifying Q2. Closer agreement is only achieved above 800mb through the addition of more complicated terms (BAL, TURB). Such complicated terms cannot be calculated simply and it would seem that no simple approximation to Q2 exists.

5. THE CLOSURE PROBLEM

The 'closure problem' refers to methods by which the net magnitude of the convective rainfall is obtained in terms of large-scale variables. Many of the methods used are empirical but most assume that some form of quasi-equilibrium exists between convection and the large-scale structure of the atmosphere. For example the Arakawa-Schubert (1974) scheme assumes a balance between the generation of moist convective instability by large-scale processes and its destruction by convection. A simplier approach was suggested by Kuo (1965, 1974) in which convection rains out a proportion of the moisture convergence coming into a column of the atmosphere. However observations show that such

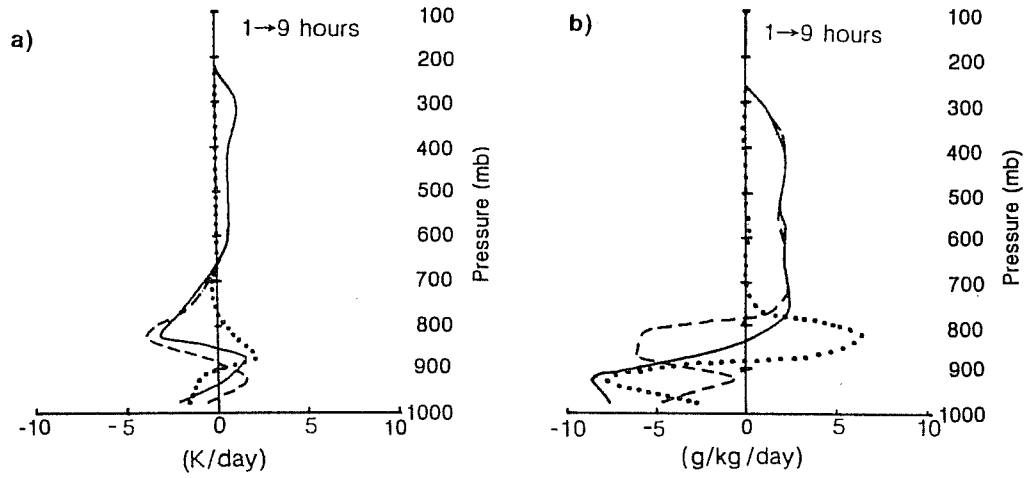

Fig. 8 Profiles of vertical eddy flux divergence (————), contribution from cloudy air (— — — —) and contribution from cloud environment (.....) for (a) T and (b) q for simulation A.

quasi-equilibrium conditions do not always exist, convection being either underactive or overactive.

For example, in the period of the TPRR data previously discussed (20-30hours; wave category three) convection rains out a large proportion of the moisture convergence into the GATE domain. This is well simulated by the model with 78% of the moisture convergence being rained out by convection. However between 0 and 10 hours of the TPRR data (wave category one) the observed rainfall rate is only one third of the moisture convergence, the remainder being stored within the atmosphere. Both the Arakawa-Schubert and Kuo schemes fail to represent such periods, overestimating the onset of active convection by up to 20 hours.

In general the processes involved in moisture storage are not well understood. Figure 9 compares the thermodynamic profiles for 2 hours and 20 hours of the TPRR data set. The 2 hour profile is warmer and drier than that of 20 hours (by up to 0.8K and 0.5g/kg), Convective Available Potential Energy (CAPE) being lower for the 2 hour profile. Also only the lowest two model layers have positive buoyancy on acsent, while the same is true of the lowest three layers for the 20 hour profile. Could these differences in thermodynamic structure modulate the response of convection to large-scale forcing. The model was used to investigate further with two further experiments being carried out (B and C - summarised in table 1).

Simulation B was initialised with the 20 hour profile (as used in simulation A), but was forced with data from category one of the wave cycle. Hence the response of convection to a forcing reduced to one third that of simulation A but with an unchanged thermodynamic structure can be studied.

Simulation C models category one of the wave cycle being initialised with the 2 hour profile and using the same forcing data as in B. Comparison with experiment B enables the impact of differing thermodynamic structure upon the convective response to large-scale forcing to be addressed.

In each experiment, the large-scale heat and moisture forcing, averaged between one and nine hours, were $-288 Wm^{-2}$ and $322 Wm^{-2}$, while surface fluxes of latent and sensible heat were $5 Wm^{-2}$ and $89 Wm^{-2}$ respectively.

For experiment B rainfall over the last 8 hours of the simulation was $300 Wm^{-2}$, approximatley 70% of the moisture convergence provided, similar to simulation A.

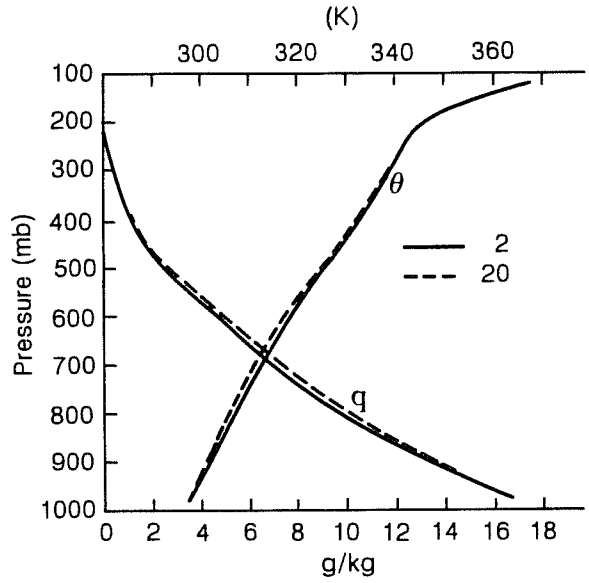

Fig. 9 Comparison of 2 and 20 hours profiles.

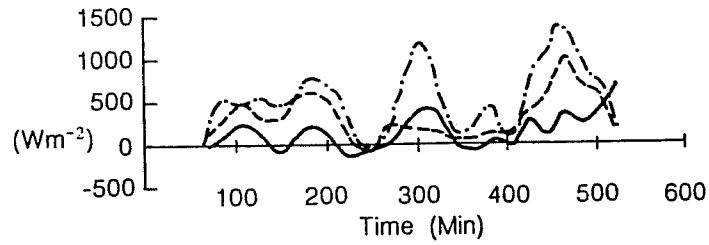

Fig. 10 Evolution of $\langle c_p \pi Q1 \rangle$ with time for simulations A (—·—·—·—), B (– – – –) and C (————).

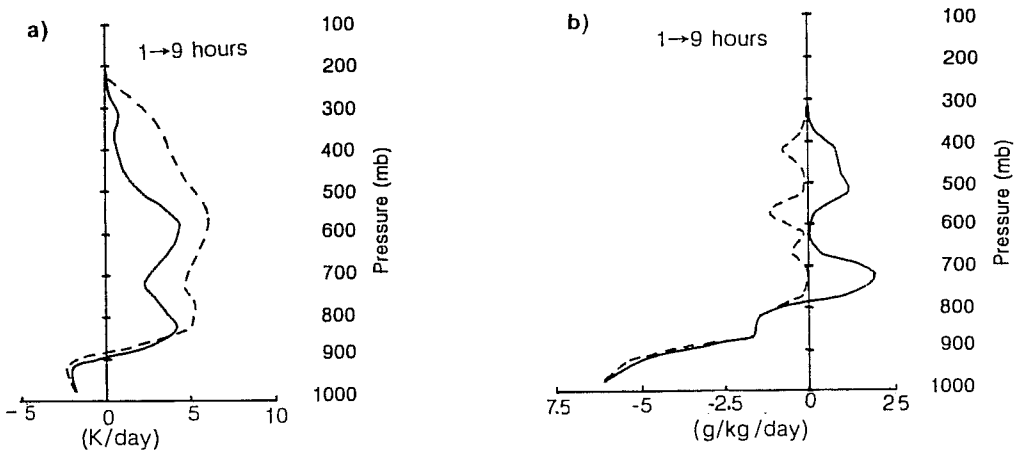

Fig. 11 Comparison of (a) Q1 and (b) Q2 for simulations B (– – – –) and C (————).

Less convection is present, the updraught area being reduced by around 30%. The decrease in convection is seen in fig 10 which shows 20-minute averages of $\langle c_p \pi Q1 \rangle$ for simulations A, B and C. For A and B, convective events are present at 100 to 200 min and 450 min. However, in B the event at 300 min is suppressed. This is perhaps not surprising as the total forcing (including radiation) is approximately half that of experiment A, requiring twice as long to destabilise the domain after the initial active convection. Hence simulation B suggests that when the initial profile is fixed, convection reacts linearly to changes in large-scale forcing, as the Kuo and Arakawa-Schubert closure hypothesis suggests.

Over the last eight hours of simulation C $\langle c_p \pi Q1 \rangle$ was 150Wm^{-2}, which compares well with the observed surface rainfall of 110Wm^{-2}. Comparison of vertical profiles of Q1 and Q2 with simulation B (fig 11) shows agreement below 800mb but a marked reduction in simulation C above this. Q2 is dominated by two layers of moistening, eddy transports dominating convective drying. Eddy transports are generally weaker, those of temperature peaking at 500mb, compared with 350mb for simulations A and B.

The results indicate that the convection in simulation C is shallower than in B and also less active, only 37% of the moisture forcing being rained out. For both simulations the large-scale forcing is identical, the difference being in their initial thermodynamic profiles. It is concluded that the thermodynamic structure of wave category one inhibits the response of convection to large-scale forcing, with resulting moisture storage.

This can be clearly seen if the evolution of $\langle Lq \rangle$ is studied. Figure 12 shows 20-minute averages of $\langle LQ/c_p \rangle$ and $\langle Lq \rangle$ for 200mb-thick layers between 1000 and 200mb, for each simulation. The lowest layer (1000 - 800mb) shows a similar evolution in both simulations, $\langle Lq \rangle$ being approximately constant compared with the input of moisture by external forcing, which is transported upward by convection. Between 800 and 600mb the atmosphere is moistened by cloud transport from below and the external forcing. The rate of moistening in simulation B is less that that due to large-scale forcing alone, indicating that much of the moisture input is rained out. For C the rate of moistening is greater than that due to large-scale forcing and hence some of the water transported into this layer from below is not rained out but stored in the atmosphere. This agrees with the layer of moistening seen in the Q2 profile (fig 11). By 5 hours, this layer contains as much water vapour as the initial

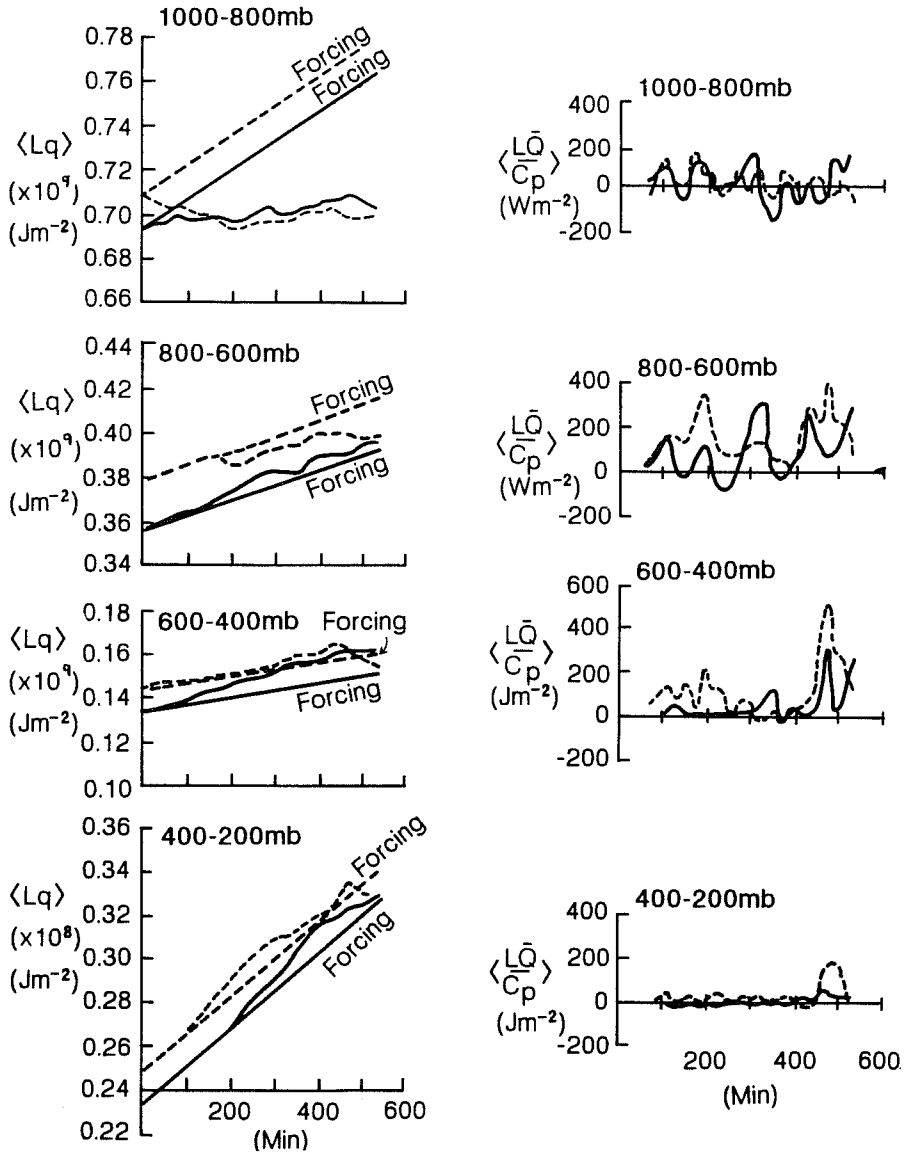

Fig. 12 Evolution of $\langle LQ/c_p \rangle$ and $\langle Lq \rangle$ with time for 200mb thick layers for simulations B(- - - -) and C (————).

profile of simulation B. Before this, the convective heating in C is only 50% that of the peak magnitude in B, whereas after 5 hours, heating rates are similar.

It should be noted that the storage is one of water vapour not liquid water. The storage of liquid water within clouds is only 10% that of the storage of water vapour in the clouds environment, agreeing with the calculations of Johnson (1980) in a study of the composite easterly wave data of TPRR.

The drier atmosphere of category one suppresses convection through the greater effect of entrainment of environmental air. As the cloud grows through a dry layer, entrainemnt causes evaporation and so reduces buoyancy. If the layer is too dry the cloud is unable to grow through it and detrains, causing moistening. The warmer profile used initially in simulation C will also aid this process, reducing buoyancy in mid-levels. Thus the model results indicate that the atmospheric thermodynamic structure modulates the response of convection to changes in the large-scale forcing.

6. THE PARAMETRISATION OF CONVECTIVE MOMENTUM TRANSPORTS

This is perhaps the most uncertain and complex part of the parametrisation of convective scale processes in large-scale numerical models. Schneider and Lindzen (1976) proposed a scheme in which horizontal momentum was assumed to be conserved during ascent in a cloud. This is commonly called 'cumulus friction' and has been implemented in several large-scale models (for example ECMWF). Observational studies however are ambiguous as to whether such transports are important. Shapiro and Stevens (1980) in a study of GATE data and Lee (1984) studying hurricane momentum budgets found that 'cumulus friction' explained the bulk of the residual in the momentum budgets. However, Thompson and Hartmann (1979) studying the Hadley circulation concluded that cumulus friction was unimportant. Also horizontal momentum is not conserved during ascent due to the presence of cloud scale pressure gradients. Several distinct types of convection are known to occur in the atmosphere, each of which has different momentum transport characteristics (Moncrieff 1981).

Two experiments were carried out to study the effects of shear upon convective parametrisation and to consider the parametrisation of momentum transports. Simulation D was identical to simulation A except it was initialised with the 20 hour zonal wind profile (fig 13). Simulation E was similar but initialised with

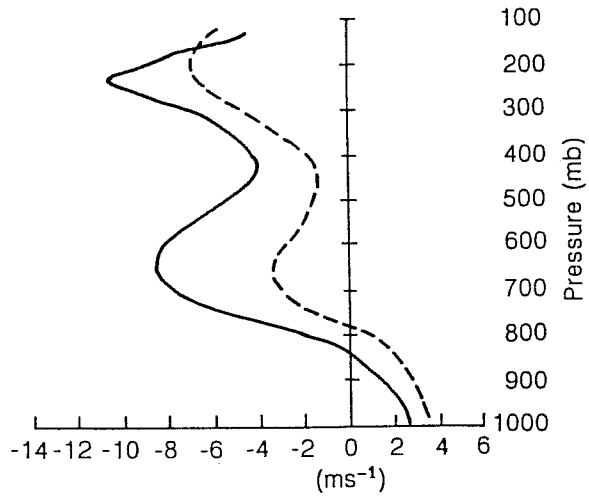

Fig. 13 Comparison of u profiles for 2 (————) and 20 (- - - -) hours.

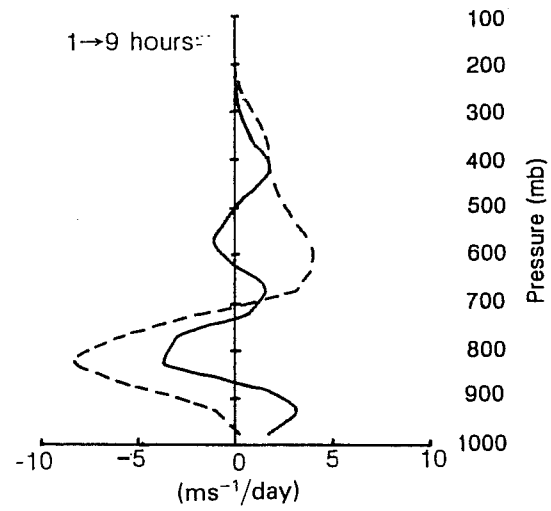

Fig. 14 Profile of vertical eddy flux divergence of u for simulations D (————) and E (- - - -).

the 2 hour zonal wind profile. Although this is an 'artificial' case in that it did not exist in reality it was carried out to study the impact of stronger shear. Both wind profiles have zonal jets around 700 and 200mb, the 2 hour profile having the stronger shear in low levels, although this is only half that associated with squall line development (15-25m/s in the lowest 200mb).

Simulation D was similar to simulation A with 495Wm^{-2} of rainfall being produced over the last 8 hours of the experiment. Below 500mb clouds travel to the west at 2m/s (the speed of the 650mb wind). At high levels the clouds move with the mean wind speed. Thus the weak low-level shear appears to induce some organisation in the lower troposphere, typical of squall lines.

The increased shear of simulation E delays the onset of convection until 200 minutes, but once formed the domain is dominated by one large convective system which propagates from east to west at the 700mb mean flow speed (8m/s). Few other clouds penetrate above 500mb. The system has squall line characteristics, with an updraught sloping against the mean wind shear and outflow ahead of and behind the storm. The downdraught forms a density current 100mb deep and 1.5K cooler than air upstream of the system, new cells forming to the west of this feature.

The system produces more rain than in simulation A or D, rainfall between one and nine hours being 650Wm^{-2}, ~90% of the applied moisture forcing. Q1 and Q2 are 2K/d and 1g/kg/d larger between 800 and 500mb than in simulation A. Internal cloud structure is similar to that of simulation A and D, apart from the in-cloud wind field. In simulation D $\tilde{u}^{UD}$ and $\tilde{u}^{DD}$ follow u relatively closely (not shown) as does $\tilde{u}^{DD}$ in simulation E. $\tilde{u}^{UD}$ in the latter experiment is ~2-3m/s slower than that in simulation D between 800 and 200mb. These results indicate that it is not possible to assume u^c is approximately conserved during ascent, as suggested by Schneider and Lindzen (1976).

Below 700mb eddy momentum transports (fig 14) act in a similar manner, accelerating the lower part of the 700mb jet to the west and in simulation D the surface flow to the east, thus increasing the low-level shear and so encouraging further organisation of the system. Differences are seen above 700mb. In D the transports correlate well with the shape of $-\partial u/\partial p$ suggesting a mixing length process. In E the flow is accelerated to the east reflecting the greater organization of convection and agreeing with the results of previous studies (e.g Miller and Betts 1977). In both simulations updraught

Fig. 15 Contribution of UD (————), DD (- - - -) and IC (·····) to vertical eddy flux divergence of u for simulation E.

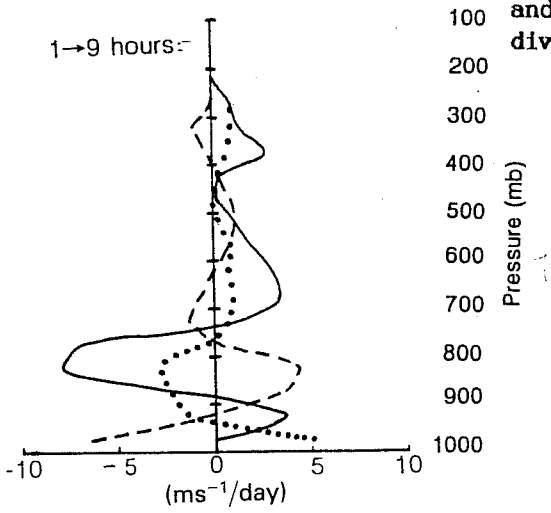

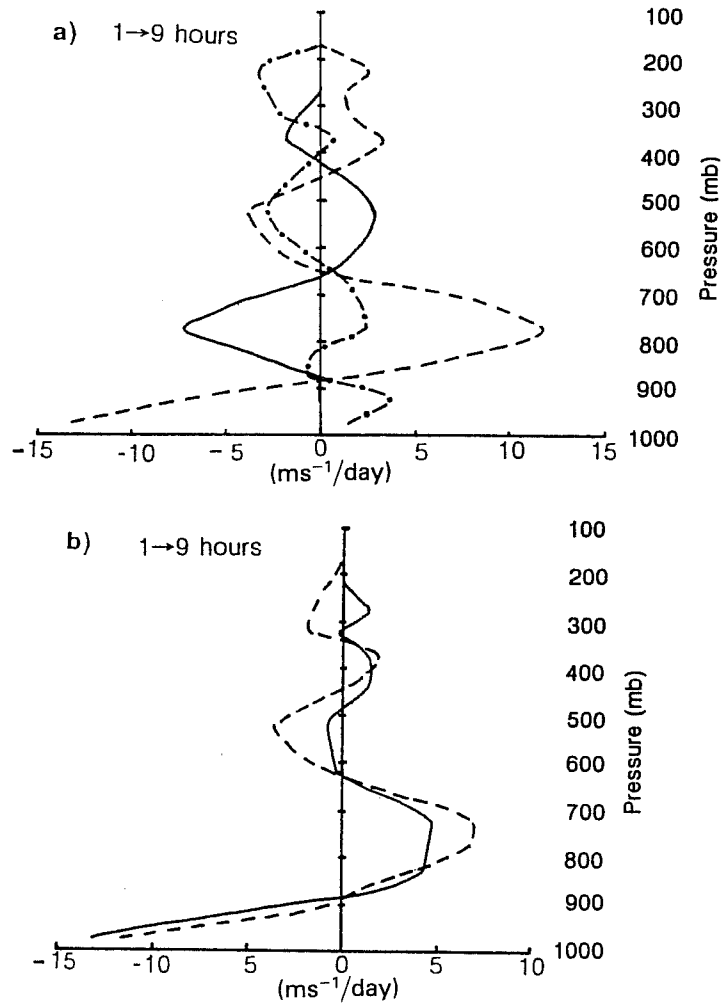

Fig. 16 Approximations to vertical eddy flux divergence of u:-
(a) $(CS)_u$ (————), $(CPG)_u$ (- - - -),
$(ADV+ED)_u$ (-·-·-·-),
(b) $(CS+CPG)_u$ (————), $(CS+CPG+ED+ADV)_u$ (- - - -)
for simulation D.

transports dominate (fig 15, simulation E), providing a reasonable representation of the transports. Downdraughts oppose updraughts below 800mb although this effect is offset somewhat by the contribution of inactive cloud.

The simple representation of Q3 by several terms in eqn(8) was considered. Figure 16(a) shows CS, cloud pressure gradient (CPG) and (ED+ADV) diagnosed from simulation D (E being similar). CS gives a poor representation of eddy transports, being of the opposite sign below 650mb. CPG is a large term and opposes CS. Their combination brings worse agreement below 650mb (fig 16(b); cf. fig 15) but better agreement above. Inclusion of (ED+ADV) brings no improvement. Hence simple terms seem unable to represent convective momentum transports and improvement only arises with the inclusion of time-dependent and boundary terms. These cannnot be obtained from simple cloud models and so the parametrisation of convective momentum transports would appear difficult.

7. DEVELOPMENT OF CONVECTION SCHEMES - AN EXAMPLE

Meso-scale convection models, as demonstrated in this paper, provide details concerning cloud structure and processes not available with any degree of accuracy from observational studies. This new source of information is valuable for the development of convective parametrisation schemes, especially for validating schemes when run in single column models.

The results of this study have been used as guidelines for the improvement of the convection scheme in use at the UK Meteorological Office in large-scale models (Gregory and Rowntree 1990), especially the inclusion of a downdraught representation into the mass flux scheme presently in use. Figure 17 shows results from a single column models forced with data from TPRR. Results are for 20-30 hours of the wave cycle, those from the cloud model being from simulation A. Without a downdraught included, the updraught balances the cooling due to large-scale forcing, being in poor agreement with the cloud model. Inclusion of a downdraught representation into the scheme brings better agreement with the results diagnosed from the cloud model, and also brings improvement to the simulated boundary layer structure and surface fluxes.

Microphysical data diagnosed from the cloud model has also been used to validate the inclusion of a Kessler microphysics scheme into scheme (fig18 - again for 20-30 hours of the wave cycle; simulation A). Both cloud and rain water are reasonable simulated. The lower peak in the rain water profile

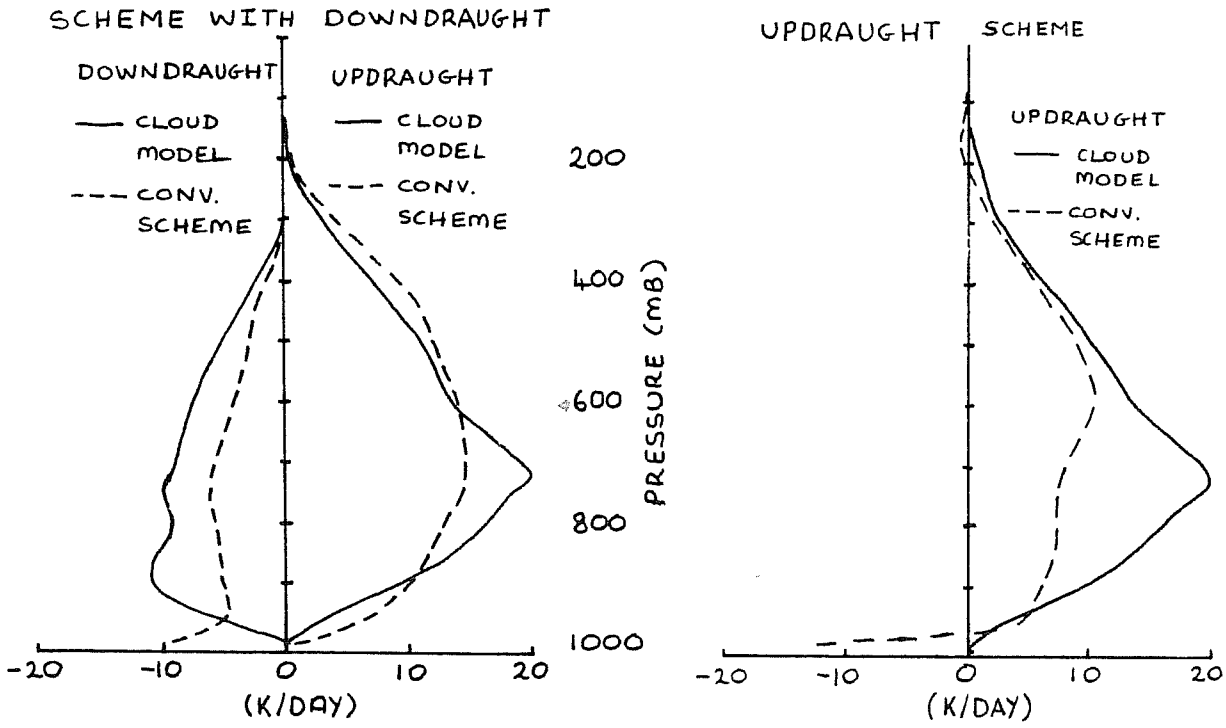

Fig. 17 Comparison of heating/cooling profiles due to updraught and downdraughts from the standard UK Met. Office convection scheme (updraughts only) and a revised (downdraughts included) scheme with those diagnosed from simulation A.

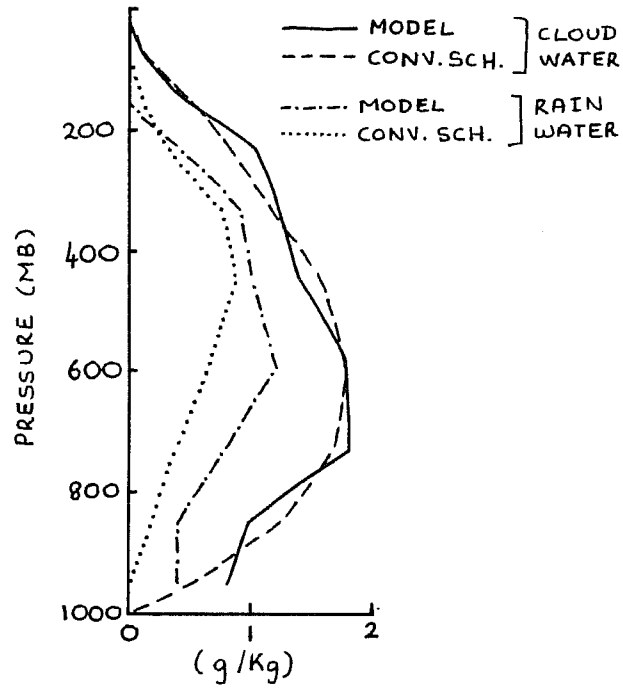

Fig 18 Comparison of cloud and rain water profiles from a revised UK Met. Office convection scheme with Kessler microphysics against values diagnosed from simulation A.

modelled by the cloud model is presumably due to falling rain which is not accounted for in the profile obtained from the parametrisation scheme.

8. SUMMARY AND CONCLUSIONS

This paper demonstrates that numerical cloud models can simulate an ensemble of convective elements and their interaction with the large-scale atmosphere, providing information on cloud-scale transports unobtainable from observational data.

The model has been used to study the problem of convective parametrisation in large-scale models, the results indicating where current parametrisation schemes must be improved in order to adequately represent convective forcing in such models. In particular, downdraughts must be included in the calculation of Q1, Q2 and Q3. Q2 would appear especially difficult to compute accurately, as is Q3, which is not well represented by the 'cumulus friction' hypothesis. The sensitivity of convection to changes in temperature and moisture structure seen in this study, emphasizes the need for more comprehensive closure schemes than are currently used. The use of the results from the cloud model to improve the physical basis of the mass flux convection scheme used in large-scale models at the UK Meteorological Office has been briefly discussed.

Owing to the difficulties of obtaining comprehensive data sets, present day convective parametrization schemes have only been tested for a few observed cases. Such models as the one used here will allow greater validation of convection schemes over a wider variety of atmospheric conditions. In particular, the latest generation of super computers enables the use of three dimensional models with increased resolution, which will provide a powerful tool for the future development of convective parametrization schemes.

9. REFERENCES

Anthes, R.A., 1977: A cumulus parametrization scheme utilizing a one-dimensional cloud model., Mon.Wea.Rev., 105, 270-286.

Arakawa, A., and Schubert, W.H., 1974: Interaction of a cumulus cloud ensemble with the large-scale environment, part I., J.Atmos.Sci., 31, 674-701.

Cox, S.K. anf Griffith, K.T., 1979: Estimates of radiative divergence during phase III of the GARP Atlantic Tropical Experiment: Part II. Analysis of phase III results., Journ.Atmos.Sci., 36, 586-601.

Gregory, D. and Miller, M.J., 1989: A numerical study of the parametrization of deep tropical convection., Quart.J.Roy.Met.Soc., 115, 1209-1241.

Gregory, D. and Rowntree, P.R., 1990: A mass flux convection scheme with representation of cloud ensemble characteristics and stability dependent closure., Mon.Wea.Rev., 118, 1483-1506.

Hill, G.E., 1974: Factors controlling the size and spacing of cumulus clouds as revealed by numerical experiments., Journ.Atmos.Sci., 31, 646-673.

Johnson, R.H., 1980: Diagnosis of convective and meso-scale motions during phase III of GATE., Journ.Atmos.Sci., 37, 733-753

Kessler, E., 1969: On the distribution and continuity of water substance in atmospheric circulations., Met.Mon., (Amer.Met.Soc), 10, No.32.

Kuo, H.L., 1965: On the formation and intensification of tropical cyclones through latent heat release by cumulus convection., Journ.Atmos.Sci., 22, 40-63

Kuo, H.L., 1974: Further studies of the parametrization of the influence of cumulus convection on large-scale flow., Journ.Atmos.Sci., 31, 1232-1240.

Lee, C-S., 1984: The bulk effects of cumulus momentum transports in tropical cyclones., Journ.Atmos.Sci., 41, 590-603.

Miller, M.J. and Betts, A.K., 1977: Travelling convective storms over Venezuela., Mon.Wea.Rev., 105, 833-848.

Miller, M.J. and Pearce, R.P., 1974: A three-dimensional primitive equation model of cumulonimbus convection., Quart.J.Roy.Met.Soc., 100, 133-154.

Moncrieff, M.W., 1981: A theory of organised steady convection and its transport properties., Quart.J.Roy.Met.Soc., 107, 29-50.

Ooyama, K., 1971: A theory on parametrization of cumulus convection., J.Met.Soc.Jap., 49 (special issue), 744-756.

Schneider, E.K., and Lindzen, R.S., 1976: A discussion of the parametrization of momentum exchange by cumulus convection., J.Geophys.Res., 81, 3158-3160.

Shapiro, L.J., and Stevens, D.E., 1980: Parametrization of convective effects on the momentum and vorticity budgets of synoptic-scale Atlantic tropical waves., Mon.Wea.Rev., 108, 1816-1826.

Tao, W-K, Simpson,J., and Soong, S-T., 1897: Statistical properties of a cloud ensemble: A numerical study., Journ.Atmos.Sci., 44, 3175-3187.

Thompson, S.L. and Hartmann, D.L., 1979: Cumulus friction: estimated influence on the tropical mean meridional circulation., Journ.Atmos.Sci., 36, 2022-2026.

Thompson, R.M., Payne, S.W., Recker, E.E., and Reed, R.J., 1979: Structure and properties of synoptic-scale wave disturbances in the intertropical convergence zone of the eastern Atlantic., Journ.Atmos.Sci., 36, 53-72

Yanai, M., Esbensen, S., and Chu, J-H., 1973: Determination of bulk properties of tropical cloud clusters from large-scale heat and moisture budgets., Journ.Atmos.Sci., 30, 611-627.